Inorganic Chemistry
Article

Inorg. Chem. **2010**, *49*, 9581–9589 **9581**
DOI: 10.1021/ic101370v

Polar or Non-Polar? Syntheses, Crystal Structures, and Optical Properties of Three New Palladium(II) Iodates

Chuan-Fu Sun,[†,‡] Chun-Li Hu,[†] Xiang Xu,[†] and Jiang-Gao Mao*,[†]

[†]*State Key Laboratory of Structural Chemistry, Fujian Institute of Research on the Structure of Matter, Chinese Academy of Sciences, Fuzhou 350002, P.R. China, and* [‡]*Graduate School of the Chinese Academy of Sciences, Beijing 100039, P.R. China*

Received July 9, 2010

Three new novel palladium(II) iodates with square-planar PdO_4 units, namely, $Pd(IO_3)_2$, $AgPd(IO_3)_3$, and $BaPd(IO_3)_4$, have been successfully hydrothermally synthesized. They represent the first ternary and quaternary palladium(II) iodates and display three different structural types. $Pd(IO_3)_2$ exhibits a novel two-dimensional (2D) layered structure in which each PdO_4 square further connects with four neighboring ones by four bridging IO_3 groups. $AgPd(IO_3)_3$ exhibits a unique three-dimensional (3D) network based on unique one-dimensional (1D) $[Pd(IO_3)_3]^-$ anionic chains along the *c*-axis which are further interconnected by Ag^+ cations. $BaPd(IO_3)_4$ is isostructural with $KAu(IO_3)_4$, and its structure features zero-dimensional (0D) $[Pd(IO_3)_4]^{2-}$ anionic units that are interconnected by Ba^{2+} cations. These materials can be polar or non-polar depending on the different alignments of the lone pairs of the I(V) atoms. $Pd(IO_3)_2$ and $AgPd(IO_3)_3$ are non-polar and centrosymmetric, hence not second-harmonic generation (SHG) active. $BaPd(IO_3)_4$ is polar and displays a moderate SHG response of about 0.4× KTP. Thermal analyses, optical, luminescent, and ferroelectric properties as well as electronic structure calculations have also been performed.

Introduction

Noncentrosymmetric (NCS) compounds, and especially the polar compounds among them, are of great interest in material science and engineering because of their interesting physical properties, such as piezoelectricity, pyroelectricity, ferroelectricity, and especially second-order nonlinear optical (NLO) properties.[1] In the past decades, much effort has been made to search for new NCS materials, and many NCS compounds have been found to be very useful NLO materials, including borates such as β-BaB_2O_4 (BBO) and LiB_3O_5 (LBO), phosphates such as KH_2PO_4 (KDP) and $KTiOPO_4$ (KTP), niobates such as $LiNbO_3$ (LN) and semiconducting materials (such as CdSe and $AgGaSe_2$).[2,3]

Metal iodates such as α-$LiIO_3$, NaI_3O_8,[4b] and $Cs_2I_4O_{11}$[4c] have been also reported to be promising NLO materials, all of them contain I(V) with a lone-pair in an asymmetric coordination geometry. They may have wide transparency regions, large second-harmonic generation (SHG) coefficients, and high optical-damage thresholds as well as good thermal stability.[4] So far, a number of ternary metal iodates have been reported; the cations used include alkali, alkaline earth, transition metal, lanthanide, and post-transition metal main group elements.[4−6] A family of actinide iodates (mostly U(VI) and Th(IV)) have also been reported by the Albrecht-Schmitt group.[7,8] Transition metal cations with d^0 electronic

---

*To whom correspondence should be addressed. E-mail: mjg@fjirsm.ac.cn.

[1] (a) Chen, C.; Liu, G. *Annu. Rev. Mater. Sci.* **1986**, *16*, 203. (b) Ok, K. M.; Halasyamani, P. S. *Chem. Soc. Rev.* **2006**, *35*, 710. (c) Halasyamani, P. S.; Poeppelmeier, K. R. *Chem. Mater.* **1998**, *10*, 2753. (d) Wickleder, M. S. *Chem. Rev.* **2002**, *102*, 2011.

[2] (a) Becker, P. *Adv. Mater.* **1998**, *10*, 979. (b) Chen, C. T.; Wang, Y. B.; Wu, B. C.; Wu, K. C.; Zeng, W. L.; Yu, L. H. *Nature* **1995**, *373*, 322. (c) Chen, C. T.; Wu, B. C.; Jiang, A. D.; You, G. M. *Sci. Sin., Ser B* **1984**, *14*, 598. (d) Hagerman, M. E.; Poeppelmeier, K. R. *Chem. Mater.* **1995**, *7*, 602. (e) Ballman, A. A.; Brown, H. *J. Cryst. Growth* **1967**, *1*, 311.

[3] (a) Dmitriev, V. G.; Gurzadyan, G. G.; Nikogosyan, D. N. *Handbook of Nonlinear Optical Crystals*; Springer: Berlin, 1991. (b) Liao, J. H.; Marking, G. M.; Hsu, K. F.; Matsushita, Y.; Ewbank, M. D.; Borwick, R.; Cunningham, P.; Rosker, M. J.; Kanatzidis, M. G. *J. Am. Chem. Soc.* **2003**, *125*, 9484. (c) Zhang, Q.; Chung, I.; Jang, J. I.; Ketterson, J. B.; Kanatzidis, M. G. *J. Am. Chem. Soc.* **2009**, *131*, 9896.

[4] (a) Rosenzweig, A.; Morosin, B. *Acta Crystallogr.* **1966**, *20*, 758. (b) Phanon, D.; Gautier-Luneau, I. *Angew. Chem., Int. Ed.* **2007**, *46*, 8488. (c) Ok, K. M.; Halasyamani, P. S. *Angew. Chem., Int. Ed.* **2004**, *43*, 5489. (d) Ok, K. M.; Halasyamani, P. S. *Inorg. Chem.* **2005**, *44*, 9353. (e) Phanon, D.; Gautier-Luneau, I. *J. Mater. Chem.* **2007**, *17*, 1123. (f) Hu, T.; Qin, L.; Kong, F.; Zhou, Y.; Mao, J. G. *Inorg. Chem.* **2009**, *48*, 2193.

[5] (a) Assefa, Z.; Ling, J.; Haire, R. G.; Albrecht-Schmitt, T. E.; Sykora, R. E. *J. Solid State Chem.* **2006**, *179*, 3653. (b) Ngo, N.; Kalachnikova, K.; Assefa, Z.; Haire, R. G.; Sykora, R. E. *J. Solid State Chem.* **2006**, *179*, 3824. (c) Sykora, R. E.; Khalifah, P.; Assefa, Z.; Albrecht-Schmitt, T. E.; Haire, R. G. *J. Solid State Chem.* **2008**, *181*, 1867.

[6] (a) Hector, A. L.; Henderson, S. J.; Levason, W.; Webster, M. *Z. Anorg. Allg. Chem.* **2002**, *628*, 198. (b) Douglas, P.; Hector, A. L.; Levason, W.; Light, M. E.; Matthews, M. L.; Webster, M. *Z. Anorg. Allg. Chem.* **2004**, *630*, 479. (c) Chen, X.; Xue, H.; Chang, X.; Zang, H.; Xiao, W. *J. Alloys Compd.* **2005**, *398*, 173. (d) Phanon, D.; Bentria, B.; Benbertal, D.; Mosset, A.; Gautier-Lunean, I. *Solid State Sci.* **2006**, *8*, 1466. (e) Masse, R.; Guitel, J. C. *J. Solid State Chem.* **1980**, *32*, 177.

configurations (such as V^{5+}, Nb^{5+}, Mo^{6+}, etc.), which are also susceptible to second-order Jahn–Teller (SOJT) distortion,[9] have been introduced into metal iodates to design and synthesize new second-order NLO materials. And many of these materials display excellent SHG responses because of the "additive" polarizations of both types of asymmetric units.[10–14] For example, $BaNbO(IO_3)_5$ displays a very large SHG response of about 14× KDP.[12a] Most of such studies have been focused on alkali, alkaline earth, and lanthanide compounds.[10–14] A few silver(I) iodates with d^0 additional transition metal cations (Ti^{4+}, V^{5+}, and Mo^{6+}) have been also reported by our group.[15] Recently, it is found that some alkali metal-transition metal iodates can also exhibit good SHG properties.[16] So far, little is known about the metal iodates in which the metal ions are in square-planar geometries such as gold(III) and palladium(II). Our hypothesis is that such square-planar geometry could also induce the formation of materials with acentric or polar structures and good NLO properties if the iodate groups are properly aligned such as being located at the same side of the MO_4 square plane. To the best of our knowledge, except for several centrosymmetric metal periodates,[17] only two such metal iodates have been reported, namely, $K_{2.5}Pd(IO_3)_4 \cdot H_{0.5}IO_3$ and $KAu(IO_3)_4$.[18] The former is centrosymmetric and hence not SHG active. The latter is polar, but unfortunately its SHG properties have not been measured. Our research efforts in the Pd–I–O systems afforded three new compounds, namely, $Pd(IO_3)_2$, $AgPd(IO_3)_3$, and $BaPd(IO_3)_4$. They belong to three different types of structures. More interestingly, $BaPd(IO_3)_4$ is the first polar palladium(II) iodate and displays a moderate SHG efficiency of about 0.4 times that of KTP ($KTiOPO_4$). Herein, we report their syntheses, crystal structures, and physical properties.

Experimental Section

Materials and Methods. All of the chemicals were analytically pure from commercial sources and used without further purification. $SrCO_3$, Ag_2O, $BaCO_3$, and I_2O_5 were purchased from the Shanghai Reagent Factory (AR, 90.0+%). $Pd(CH_3COO)_2$ and aqueous solution of $Pd(NO_3)_2 \cdot 2H_2O$ (1 g/10 mL) were purchased from Shanghai Jiuyue Reagent Factory (AR, 90.0+%). IR spectra were recorded on a Magna 750 FT-IR spectrometer as KBr pellets in the range of 4000–400 cm^{-1}. Microprobe elemental analyses were performed on a field emission scanning electron microscope (FESEM, JSM6700F) equipped with an energy dispersive X-ray spectroscope (EDS, Oxford INCA). X-ray powder diffraction (XRD) patterns were collected on a Panalytical X'pert Pro MPD diffractometer using graphite-monochromated Cu–Kα radiation in the 2θ range of 5–80° with a step size of 0.02°. Optical diffuse reflectance spectra were measured at room temperature with a PE Lambda 900 UV–visible spectrophotometer. $BaSO_4$ plate was used as a standard (100% reflectance). The absorption spectrum was calculated from reflectance spectra using the Kubelka–Munk function: $\alpha/S = (1 - R)^2/2R$,[19] where α is the absorption coefficient, S is the scattering coefficient which is practically wavelength independent when the particle size is larger than 5 μm, and R is the reflectance. Thermogravimetric analyses were carried out with a NETZSCH STA 449C unit at a heating rate of 10 °C/min under a N_2 atmosphere. Photoluminescence spectra were recorded on a Perkin-Elmer LS55 fluorescence spectrometer. The measurements of SHG were carried out on the sieved (70–100 mesh) powder samples of $BaPd(IO_3)_4$ by using the Kurtz and Perry method with a 2.05 μm Q-switch laser.[20] The sieved KTP powders (70–100 mesh) were used as reference materials to assume the effect. The ferroelectric measurements were performed using an aixACCT TF Analyzer 2000 ferroelectric tester at room temperature. The sample was pressed into a pellet (5-mm-diameter and 0.8-mm-thick), and the conducting Ag-glue was applied on the both sides of the pellet surfaces for electrodes.

Preparation of $Pd(IO_3)_2$. A mixture of $SrCO_3$ (0.0148 g, 0.10 mmol), $Pd(CH_3COO)_2$ (0.0225 g, 0.10 mmol), I_2O_5 (0.6676 g, 2.00 mmol), and H_2O (2.0 mL) was sealed in an autoclave equipped with a Teflon linear (23 mL) and heated at 200 °C for 4 days, followed by slow cooling to room temperature at a rate of 6 °C/h. Red plate-shaped crystals of $Pd(IO_3)_2$ were obtained along with colorless plate-shaped $Sr(IO_3)_2$ crystals as impurities. After proper structural analyses, single phase of $Pd(IO_3)_2$ were obtained by the reactions of Li_2CO_3 (0.0369 g, 0.50 mmol), aqueous solution of $Pd(NO_3)_2 \cdot 2H_2O$ (1 g/10 mL) (0.2890 g, 0.10 mmol), I_2O_5 (0.6676 g, 2.00 mmol), and H_2O (2.0 mL) under the same reaction conditions mentioned above, with a yield of about 90% based on Pd. Its purity was confirmed by XRD studies (Supporting Information). Li_2CO_3 was used to mediate the pH values of the reaction solutions; it can be easily separated from water-insoluble $Pd(IO_3)_2$ because $LiIO_3$ is water-soluble. The energy-dispersive spectrometry (EDS) elemental analyses on several single crystals of $Pd(IO_3)_2$ gave an average molar ratio of Pd/I of 1.1:2.0, which is in good agreement with the one determined from single-crystal X-ray structural studies. IR data (KBr cm^{-1}): 795 (m), 764 (w), 741 (s), 675 (s), 488 (s), 409 (m).

---

(7) (a) Bean, A. C.; Campana, C. F.; Kwon, O.; Albrecht-Schmitt, T. E. *J. Am. Chem. Soc.* **2001**, *123*, 8806. (b) Bean, A. C.; Peper, S. M.; Albrecht-Schmitt, T. E. *Chem. Mater.* **2001**, *13*, 1266. (c) Ling, J.; Albrecht-Schmitt, T. E. *Inorg. Chem.* **2007**, *46*, 346. (d) Sykora, R. E.; Wells, D. M.; Albrecht-Schmitt, T. E. *Inorg. Chem.* **2002**, *41*, 2304. (e) Bray, T. H.; Beitz, J. V.; Bean, A. C.; Yu, Y.; Albrecht-Schmitt, T. E. *Inorg. Chem.* **2006**, *45*, 8251. (f) Bean, A. C.; Ruf, M.; Albrecht-Schmitt, T. E. *Inorg. Chem.* **2001**, *40*, 3959.

(8) (a) Sykora, R. E.; McDaniel, S. M.; Wells, D. M.; Albrecht-Schmitt, T. E. *Inorg. Chem.* **2002**, *41*, 5126. (b) Bean, A. C.; Xu, Y.; Danis, J. A.; Albrecht-Schmitt, T. E. *Inorg. Chem.* **2002**, *41*, 6775. (c) Sykora, R. E.; Bean, A. C.; Scott, B. L.; Runde, W.; Albrecht-Schmitt, T. E. *J. Solid State Chem.* **2004**, *177*, 725. (d) Sullens, T. A.; Almond, P. M.; Byrd, J. A.; Beitz, J. V.; Bray, T. H.; Albrecht-Schmitt, T. E. *J. Solid State Chem.* **2006**, *179*, 1192. (e) Bean, A. C.; Albrecht-Schmitt, T. E. *J. Solid State Chem.* **2001**, *161*, 416.

(9) (a) Goodenough, J. B. *Annu. Rev. Mater. Sci.* **1998**, *28*, 1. (b) Kunz, M.; Brown, I. D. *J. Solid State Chem.* **1995**, *115*, 395. (c) Halasyamani, P. S. *Chem. Mater.* **2004**, *16*, 3586. (d) Ok, K. M.; Halasyamani, P. S. *Chem. Mater.* **2006**, *18*, 3176.

(10) (a) Sykora, R. E.; Ok, K. M.; Halasyamani, P. S.; Albrecht-Schmitt, T. E. *J. Am. Chem. Soc.* **2002**, *124*, 1951. (b) Sykora, R. E.; Ok, K. M.; Halasyamani, P. S.; Wells, D. M.; Albrecht-Schmitt, T. E. *Chem. Mater.* **2002**, *14*, 2741. (c) Chen, X.; Zhang, L.; Chang, X.; Xue, H.; Zang, H. G.; Xiao, W. Q.; Song, X.; Yan, H. *J. Alloy. Compd.* **2007**, *428*, 54.

(11) (a) Chang, H. Y.; Kim, S. H.; Halasyamani, P. S.; Ok, K. M. *J. Am. Chem. Soc.* **2009**, *131*, 2426. (b) Chang, H. Y.; Kim, S. H.; Ok, K. M.; Halasyamani, P. S. *J. Am. Chem. Soc.* **2009**, *131*, 6865.

(12) (a) Sun, C. F.; Hu, C. L.; Xu, X.; Ling, J. B.; Hu, T.; Kong, F.; Long, X. F.; Mao, J. G. *J. Am. Chem. Soc.* **2009**, *131*, 9486. (b) Yang, B. P.; Hu, C. L.; Xu, X.; Sun, C. F.; Zhang, J. H.; Mao, J. G. *Chem. Mater.* **2010**, *22*, 1545.

(13) (a) Shehee, T. C.; Sykora, R. E.; Ok, K. M.; Halasyamani, P. S.; Albrecht-Schmitt, T. E. *Inorg. Chem.* **2003**, *42*, 457. (b) Chen, X.; Chang, X. N.; Zang, H. G.; Xiao, W. Q. *J. Alloy. Compd.* **2005**, *396*, 255.

(14) (a) Ok, K. M.; Halasyamani, P. S. *Inorg. Chem.* **2005**, *44*, 2263. (b) Sykora, R. E.; Wells, D. M.; Albrecht-Schmitt, T. E. *J. Solid State Chem.* **2002**, *166*, 442. (c) Sun, C. F.; Hu, T.; Xu, X.; Mao, J. G. *Dalton Trans.* **2010**, in press.

(15) Sun, C. F.; Hu, C. L.; Kong, F.; Yang, B. P.; Mao, J. G. *Dalton Trans.* **2010**, *39*, 1473.

(16) Li, P. X.; Hu, C. L.; Xu, X.; Wang, R. Y.; Sun, C. F.; Mao, J. G. *Inorg. Chem.* **2010**, *49*, 4599.

(17) (a) Dengel, A. C.; Elhendawy, A. M.; Griffith, W. P.; Mostafa, S. I.; Williams, D. J. *Dalton Trans.* **1992**, 3489. (b) Hector, A. L.; Levason, W.; Webster, M. *Inorg. Chim. Acta* **2003**, *343*, 90.

(18) Ling, J.; Albrecht-Schmitt, T. E. *Eur. J. Inorg. Chem.* **2007**, *5*, 652.

(19) Wendlandt, W. M.; Hecht, H. G. *Reflectance Spectroscopy*; Interscience: New York, 1966.

(20) Kurtz, S. W.; Perry, T. T. *J. Appl. Phys.* **1968**, *39*, 3798.

Preparation of $AgPd(IO_3)_3$. A mixture of Ag_2O (0.0115 g, 0.05 mmol), $Pd(CH_3COO)_2$ (0.0229 g, 0.102 mmol), I_2O_5 (0.6676 g, 2.00 mmol), and H_2O (2.0 mL) was sealed in an autoclave equipped with a Teflon linear (23 mL) and heated at 200 °C for 4 days, followed by slow cooling to room temperature at a rate of 6 °C/h. The product was washed with hot water and ethanol, and then dried in air. Red plate-shaped crystals of $AgPd(IO_3)_3$ were obtained as a single phase in a yield of about 85% based on Ag. Its purity was confirmed by XRD studies (Supporting Information). The energy-dispersive spectrometry (EDS) elemental analyses on several single crystals of $AgPd(IO_3)_3$ gave an average molar ratio of Ag/Pd/I of 1.0:1.1:3.2, which is in good agreement with the one determined from single-crystal X-ray structural studies. IR data (KBr cm^{-1}): 837 (m), 795 (m), 775 (s), 756 (m), 719 (s), 681 (s), 650 (s), 503 (s).

Preparation of $BaPd(IO_3)_4$. A mixture of $BaCO_3$ (0.0197 g, 0.10 mmol), $Pd(CH_3COO)_2$ (0.0234 g, 0.103 mmol), I_2O_5 (0.6676 g, 2.00 mmol), and H_2O (2.0 mL) was sealed in an autoclave equipped with a Teflon linear (23 mL) and heated at 200 °C for 4 days, followed by slow cooling to room temperature at a rate of 6 °C/h. The product was washed with hot water and ethanol, and then dried in air. Red block-shaped crystals of $BaPd(IO_3)_4$ were obtained as a single phase in a yield of about 86% based on Ba. Its purity was confirmed by XRD studies (Supporting Information). The energy-dispersive spectrometry (EDS) elemental analyses on several single crystals of $BaPd(IO_3)_4$ gave an average molar ratio of Ba/Pd/I of 1.0:1.1:3.9, which is in good agreement with the one determined from single-crystal X-ray structural studies. IR data (KBr cm^{-1}): 793 (s), 771 (s), 752 (m), 690 (s), 665 (s), 499 (s).

Single-Crystal Structure Determination. Data collections for single crystals of $Pd(IO_3)_2$, $AgPd(IO_3)_3$, and $BaPd(IO_3)_4$ with dimensions of $0.08 \times 0.07 \times 0.05$ mm^3, $0.12 \times 0.10 \times 0.09$ mm^3, and $0.08 \times 0.04 \times 0.03$ mm^3 were performed on a Rigaku SCXMini CCD diffractometer equipped with a graphite-monochromated Mo−Kα radiation (λ = 0.71073 Å) at 293(2) K. The data sets were corrected for Lorentz and polarization factors as well as for absorption by Multiscan method.[21a] All three structures were solved by the direct methods and refined by full-matrix least-squares fitting on F^2 by SHELX-97.[21b] The Flack factor of 0.29(8) for $BaPd(IO_3)_4$ indicates the existence of some extent of the racemic twinning for the sample. Crystallographic data and structural refinements for the three compounds are summarized in Table 1. Important bond distances are listed in Table 2. More details on the crystallographic studies are given as Supporting Information.

Table 1. Crystal Data and Structural Refinements for the Three Compounds

formula	$Pd(IO_3)_2$	$AgPd(IO_3)_3$	$BaPd(IO_3)_4$
Fw	456.20	738.97	943.33
crystal system	orthorhombic	triclinic	triclinic
space group	*Pbca*	$P\overline{1}$	$P1$
a/Å	5.839(3)	7.315(5)	5.7529(17)
b/Å	6.037(3)	7.991(6)	7.330(2)
c/Å	15.071(9)	8.575(5)	8.119(3)
α/deg	90	63.75(2)	105.491(4)
β/deg	90	76.59(3)	94.387(10)
γ/deg	90	82.27(3)	112.421(9)
V/Å^3	531.3(5)	437.0(5)	298.81(17)
Z	4	2	1
D_{calcd}/g·cm^{-3}	5.703	5.616	5.242
μ(Mo−Kα)/mm^{-1}	15.069	14.921	15.167
GOF on F^2	1.050	0.962	1.054
Flack factor	N/A	N/A	0.29(8)
R1, wR2 ($I > 2\sigma(I)$)[a]	0.0263, 0.0583	0.0218, 0.0484	0.0360, 0.0966
R1, wR2 (all data)	0.0310,0.0600	0.0271,0.0499	0.0366,0.0972

[a] $R1 = \sum||F_o| - |F_c||/\sum|F_o|$, $wR2 = \{\sum w(F_o^2 - F_c^2)^2/\sum w(F_o^2)^2\}^{1/2}$.

Table 2. Important Bond Lengths (Å) and Angles (deg) for the Three Compounds

	$Pd(IO_3)_2$[a]		
Pd(1)−O(3)#1	2.005(4)	Pd(1)−O(3)#2	2.005(4)
Pd(1)−O(1)	2.013(5)	Pd(1)−O(1)#3	2.013(5)
I(1)−O(1)	1.848(5)	I(1)−O(2)	1.807(5)
I(1)−O(3)	1.804(5)		
O(1)−Pd(1)−O(3)#1	91.45(19)	O(1)−Pd(1)−O(3)#2	88.55(19)
	$AgPd(IO_3)_3$[b]		
Ag(1)−O(1)#1	2.645(5)	Ag(1)−O(4)#2	2.915(6)
Ag(1)−O(5)#3	2.809(6)	Ag(1)−O(6)#4	2.516(5)
Ag(1)−O(7)#2	2.836(6)	Ag(1)−O(8)#2	2.505(6)
Ag(1)−O(9)#5	2.322(5)	Pd(1)−O(1)	2.010(5)
Pd(1)−O(1)#2	2.010(5)	Pd(1)−O(4)	2.013(5)
Pd(1)−O(4)#2	2.013(5)	Pd(2)−O(2)	2.004(5)
Pd(2)−O(2)#6	2.004(5)	Pd(2)−O(7)	2.020(5)
Pd(2)−O(7)#6	2.020(5)	I(1)−O(1)	1.846(5)
I(1)−O(2)	1.841(5)	I(1)−O(3)	1.775(6)
I(2)−O(4)	1.876(6)	I(2)−O(5)	1.791(5)
I(2)−O(6)	1.792(5)	I(3)−O(7)	1.856(5)
I(3)−O(8)	1.793(5)	I(3)−O(9)	1.813(5)
O(1)−Pd(1)−O(4)	91.7(2)	O(1)#2-Pd(1)−O(4)	88.3(2)
O(2)−Pd(2)−O(7)	90.9(2)	O(2)#6-Pd(2)−O(7)	89.1(2)
	$BaPd(IO_3)_4$		
Pd(1)−O(1)	2.018(11)	Pd(1)−O(4)	2.021(11)
Pd(1)−O(7)	1.987(11)	Pd(1)−O(10)	2.022(11)
I(1)−O(1)	1.856(11)	I(1)−O(2)	1.787(13)
I(1)−O(3)	1.806(11)	I(2)−O(4)	1.842(10)
I(2)−O(5)	1.804(13)	I(2)−O(6)	1.801(12)
I(3)−O(7)	1.837(14)	I(3)−O(8)	1.811(11)
I(3)−O(9)	1.836(13)	I(4)−O(10)	1.827(13)
I(4)−O(11)	1.793(14)	I(4)−O(12)	1.822(11)
O(1)−Pd(1)−O(4)	93.5(4)	O(1)−Pd(1)−O(7)	173.7(5)
O(1)−Pd(1)−O(10)	85.2(4)	O(4)−Pd(1)−O(7)	89.0(5)
O(4)−Pd(1)−O(10)	178.3(5)	O(7)−Pd(1)−O(10)	92.2(5)

[a] Symmetry transformations used to generate equivalent atoms. For $Pd(IO_3)_2$: #1 $-x+1/2, y+1/2, z$; #2 $x-1/2, -y+3/2, -z+1$; #3 $-x, -y+2, -z+1$. [b] Symmetry transformations used to generate equivalent atoms. For $AgPd(IO_3)_3$: #1 x, y, z; #2 $-x, -y, -z+1$; #3 $x, y-1, z+1$; #4 $-x-1, -y, -z+1$; #5 $x-1, y, z+1$; #6 $-x, -y, -z$.

Computational Descriptions. Single crystal structural data of the three compounds were used for the theoretical calculations. Band structures and density of states (DOS) were performed with the total-energy code CASTEP.[22] The total energy is calculated with density functional theory (DFT) using the Perdew−Burke−Ernzerhof (PBE) generalized gradient approximation.[23] The interactions between the ionic cores and the electrons were described by the norm-conserving pseudopotential.[24] The following orbital electrons were treated as valence electrons: Ag-$4d^{10}5s^1$, Ba-$5s^25p^66s^2$, Pd-$4d^{10}$, I-$5s^25p^5$ and O-$2s^22p^4$. The numbers of plane waves included in the basis sets were determined by a cutoff energy of 500 eV for all three compounds, and the numerical integration of the Brillouin zone is performed using a $4 \times 4 \times 2$, $4 \times 3 \times 3$, $5 \times 4 \times 3$ for $Pd(IO_3)_2$, $AgPd(IO_3)_3$, and $BaPd(IO_3)_4$, respectively. The spin polarized model was chosen to deal with the Pd^{2+} ions with d^8 electronic configuration in all three compounds. The other parameters and convergent criteria were the default values of the CASTEP code.

---

(21) (a) *CrystalClear*, Version 1.3.5; Rigaku Corp.: Woodlands, TX, 1999. (b) Sheldrick, G. M. *SHELXTL, Crystallographic Software Package*, , Version 5.1; Bruker-AXS: Madison, WI, 1998.

(22) (a) Segall, M. D.; Lindan, P. J. D.; Probert, M. J.; Pickard, C. J.; Hasnip, P. J.; Clark, S. J.; Payne, M. C. *J. Phys.: Condens. Matter* **2002**, *14*, 2717. (b) Milman, V.; Winkler, B.; White, J. A.; Pickard, C. J.; Payne, M. C.; Akhmatskaya, E. V.; Nobes, R. H. *Int. J. Quantum Chem.* **2000**, *77*, 895.

(23) Perdew, J. P.; Burke, K.; Ernzerhof, M. *Phys. Rev. Lett.* **1996**, *77*, 3865.

(24) Lin, J. S.; Qteish, A.; Payne, M. C.; Heine, V. *Phys. Rev. B* **1993**, *47*, 4174.

Results and Discussion

Three new novel palladium(II) iodates with square-planar PdO_4 units, namely, $Pd(IO_3)_2$, $AgPd(IO_3)_3$, and $BaPd(IO_3)_4$, have been successfully synthesized through hydrothermal reactions. They represent the first examples of ternary and quaternary palladium(II) iodates. They exhibit three different types of structures. It is found that the starting materials are very important for preparation of $Pd(IO_3)_2$. When $Pd(CH_3COO)_2$ was used instead of $Pd(NO_3)_2 \cdot 2H_2O$ or Li_2CO_3 is not added, the single phase of $Pd(IO_3)_2$ can not be obtained. Besides, $Pd(CH_3COO)_2$ should be in slightly excess for the preparations of $AgPd(IO_3)_3$ and $BaPd(IO_3)_4$, otherwise, $AgIO_3$ or $Ba(IO_3)_2$ impurities would also appear.

Crystal Structures. $Pd(IO_3)_2$ exhibits a novel two-dimensional (2D) layered structure in which each PdO_4 square is further interconnected with four neighboring ones by four bridging IO_3 groups (Figure 1). The Pd^{2+} cation lying on an inversion center is bonded to four oxygen atoms [$2 \times O(1)$ and $2 \times O(3)$] from four iodate anions in a square planar environment (Figure 1c). The Pd−O bond distances are 2.013(5) and 2.005(4) Å, respectively. The O(1)−Pd(1)−O(3) angles are 88.55 and 91.45° (see Table 2). Hence, the PdO_4 square unit is slightly distorted. The four iodate groups are arranged on the opposite sides of the PdO_4 plane. The four I(V) atoms are ± 1.094 and ± 0.968 Å away from the PdO_4 plane, respectively. The I(V) atom is asymmetrically coordinated by three oxygen atoms in a distorted trigonal-pyramidal environment as a result of its stereoactive lone pair, with I−O bond distances ranging from 1.804(5) to 1.848(5) Å, which are comparable to those previously reported for other metal iodates.[10−14] Results of bond valence calculations indicate that the Pd and I atoms are in an oxidation of +2 and +5, respectively. The calculated total bond valences are 2.22 and 4.93 for Pd(1) and I(1), respectively.[25]

The interconnection of the PdO_4 square units via bridging IO_3 groups results in a 2D layer perpendicular to the *c*-axis. Each Pd^{2+} cation is linked with four IO_3 groups, and each IO_3 group connects with two Pd^{2+} cations in a unidentate fashion with the third oxygen atom left non-coordinated (Figure 1b). The distance between two Pd^{2+} cations bridged by one IO_3 group within the 2D layer is 4.199(2) Å, and the shortest interlayer Pd···Pd distance is 8.081(4) Å.

In $Pd(IO_3)_2$, the lone pairs on IO_3 polyhedra are aligned trans to each other (oriented in opposite directions) (Figure 1c), which results in the cancellation of the local dipole moments, rendering the material non-polar.

The structure of $AgPd(IO_3)_3$ features a novel three-dimensional (3D) network based on unique one-dimensional (1D) $[Pd(IO_3)_3]^-$ anionic chains along the *c*-axis which are further interconnected by Ag^+ cations (Figure 2a). Its asymmetric unit contains two Pd^{2+} cations both lying on an inversion center, one Ag^+ and three I^{5+} cations in the general positions. Both Pd^{2+} cations are in a square planar environment, being coordinated by four oxygen atoms from four IO_3 groups. The Pd−O bond distances range from 2.004(5) to 2.020(5) Å, which are comparable to those in $Pd(IO_3)_2$ and $K_{2.5}[Pd(IO_3)_4] \cdot H_{0.5}IO_3$.[18] Similar to those in $Pd(IO_3)_2$, slight distortions of the square planar coordination are also found with O(1)−Pd(1)−O(4) angles of 91.7 and 88.3°, and O(2)−Pd(2)−O(7) angles of 90.9 and 89.1°, respectively

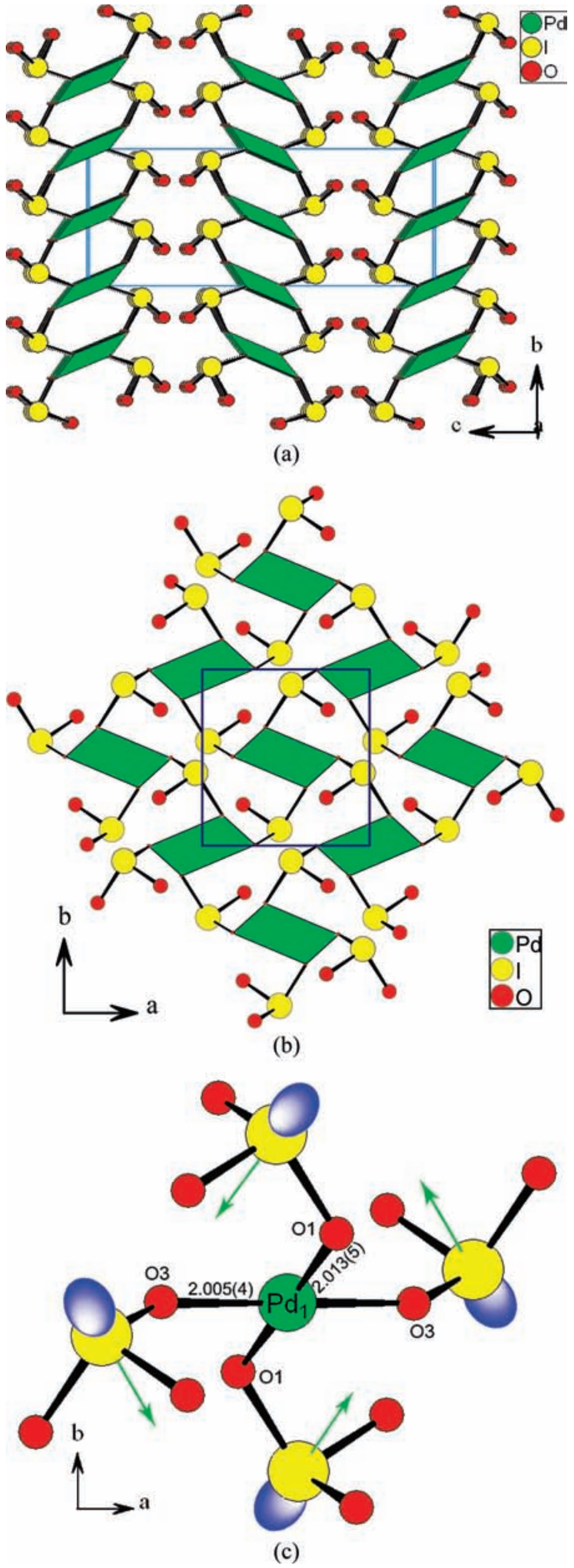

Figure 1. View of the structure of $Pd(IO_3)_2$ down the *a*-axis (a); a 2D $Pd(IO_3)_2$ layer perpendicular to the *c*-axis (b); a $[Pd(IO_3)_3]^-$ unit with the lone pairs (blue ellipsoids) and local moments (green arrows) (c). PdO_4 squares are shaded in green.

---

(25) (a) Brown, I. D.; Altermatt, D. *Acta Crystallogr.* **1985**, *B41*, 244. (b) Brese, N. E.; O'Keeffe, M. *Acta Crystallogr.* **1991**, *B47*, 192.

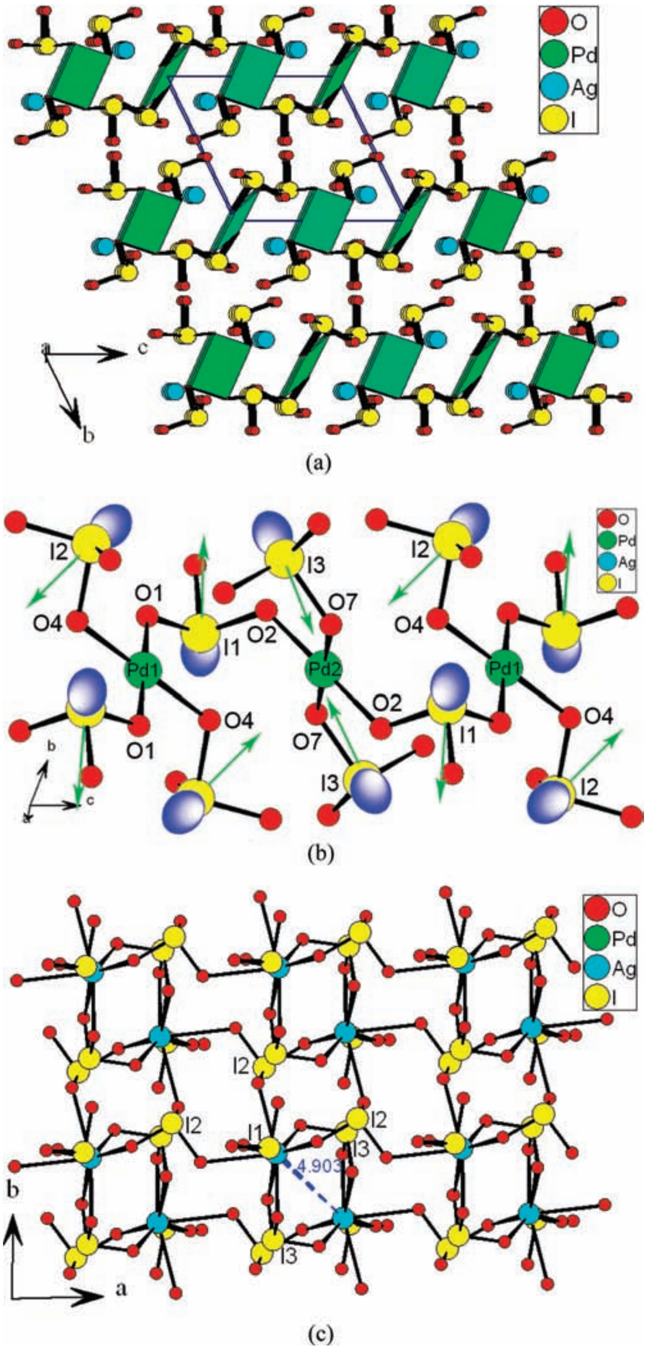

Figure 2. View of the structure of $AgPd(IO_3)_3$ down the *a*-axis (Ag−O bonds were omitted for clarity) (a); a 1D $[Pd(IO_3)_3]^-$ chain along the *c*-axis with the lone pairs (blue ellipsoids) and local moments (green arrows) (b); and a 2D $[Ag(IO_3)_3]^{2-}$ layer perpendicular to the *c*-axis (c). PdO_4 squares are shaded in green.

(see Table 2). The four iodate groups are arranged on the opposite sides of the $Pd(1)O_4$ or $Pd(2)O_4$ plane, which is similar to those in $Pd(IO_3)_2$. The I(V) atoms are away from the $Pd(1)O_4$ or $Pd(2)O_4$ plane ±0.037, ± 1.460, ± 1.043, and ±0.016 Å, respectively. Therefore two I(V) atoms are almost located on the PdO_4 plane whereas the other two I(V) atoms are arranged above and below the PdO_4 plane, which is different from those in $Pd(IO_3)_2$. The $Pd(1)O_4$ and $Pd(2)O_4$ squares are further interconnected by bridging $I(1)O_3$ groups into a unique 1D $[Pd(IO_3)_3]^-$ anionic chain along the *c*-axis (Figure 2b). $I(2)O_3$ and $I(3)O_3$ groups are alternately attached on both sides of the chain in a unidentate fashion. The distance between two neighboring Pd^{2+} cations is 4.287(3) Å, which is comparable to that in $Pd(IO_3)_2$. All three I(V) atoms are asymmetrically coordinated by three oxygen atoms in a distorted trigonal-pyramidal environment. The I−O bond distances fall in the range of 1.775(6) to 1.876(6) Å, which are comparable to those reported in other metal iodates.[4−9] Within the 1D $[Pd(IO_3)_3]^-$ anionic chain, the lone pairs of the IO_3 polyhedra are aligned trans to each other because of the presence of an inversion center in the $P\overline{1}$ space group, resulting in the cancellation of the local dipole moments (see Figure 2b) and rendering a 1D $[Pd(IO_3)_3]^-$ unit non-polar.

The Ag^+ cation is seven-coordinated by oxygen atoms from one bidentate and five unidentate IO_3 groups with Ag−O bond distances in the range of 2.322(5) to 2.915(6) Å, which are close to those reported in other silver iodates.[6e,15] Bond valence calculations,[25] resulting in values of 0.92 for Ag, 2.21 for Pd, and 4.92−4.95 for I, indicate that the Ag, Pd, and I atoms are in oxidation states of +1, +2, and +5, respectively. The silver(I) cations are interconnected by bridging iodate groups into a 2D $[Ag(IO_3)_3]^{2-}$ anionic layer perpendicular to the *c*-axis (Figure 2c). Each $I(2)O_3$ group connects with three Ag^+ cations in a unidentate fashion and each $I(3)O_3$ group connects with two Ag^+ cations in unidentate and bidentate fashions, whereas all $I(1)O_3$ groups are attached on the same side of the layer unidentately. Such anionic layer is very different from the $[Ag(IO_3)_2]^-$ anionic layer in $Ag_2(MoO_2)(IO_3)_4$,[15] in which the silver(I) cations are interconnected by bridging oxygen atoms besides bridging iodate groups. As a result, the nearest Ag···Ag distance (4.903 Å) in the former layer is much larger than that (3.492 Å) in the latter one. Hence, the structure of $AgPd(IO_3)_3$ can also be described as a 3D network based on $[Ag(IO_3)_3]^{2-}$ layers that are further interconnected by PdO_4 squares via I−O−Pd bridges (Figure 2a).

$BaPd(IO_3)_4$ is isostructural with $KAu(IO_3)_4$ in which the K^+ and Au^{3+} cations being replaced by Ba^{2+} and Pd^{2+} cations, respectively.[18] Its structure contains a zero-dimensional (0D) $[Pd(IO_3)_4]^{2-}$ anionic unit composed of one PdO_4 square linked with four IO_3 groups in a unidentate fashion (Figure 3b). Such 0D $[Pd(IO_3)_4]^{2-}$ anionic units are further interconnected into a 3D network by Ba^{2+} cations (Figure 3a).

The palladium(II) cation is in a square planar coordination environment coordinated by four oxygen atoms from four IO_3 groups, with Pd−O bond distances ranging from 1.987(11) to 2.022(11) Å. The PdO_4 square is also slightly distorted with O(1)−Pd(1)−O(4), O(4)−Pd(1)−O(7), and O(1)−Pd(1)−O(7) angles of 93.5, 89.0, and 173.7°, respectively; and O(1)−Pd(1)−O(10), O(7)−Pd(1)−O(10), and O(4)−Pd(1)−O(10) angles of 85.2, 92.2, and 178.3°, respectively (see Table 2). Hence the PdO_4 square plane in $BaPd(IO_3)_4$ is much more distorted compared with those in $Pd(IO_3)_2$ and $AgPd(IO_3)_3$. The displacement of the deviation was found to be 0.061 Å. All four I(V) atoms in the asymmetric unit are coordinated by three oxygen atoms in a distorted trigonal-pyramidal geometry. The I−O bond distances fall in the normal range of 1.787(13) to 1.856(11) Å. It is worth mentioning that all of the IO_3 groups in the 0D $[Pd(IO_3)_4]^{2-}$ anionic unit are aligned on the same side of the distorted PdO_4 square with all of the lone pairs on I(V) cations oriented in almost the

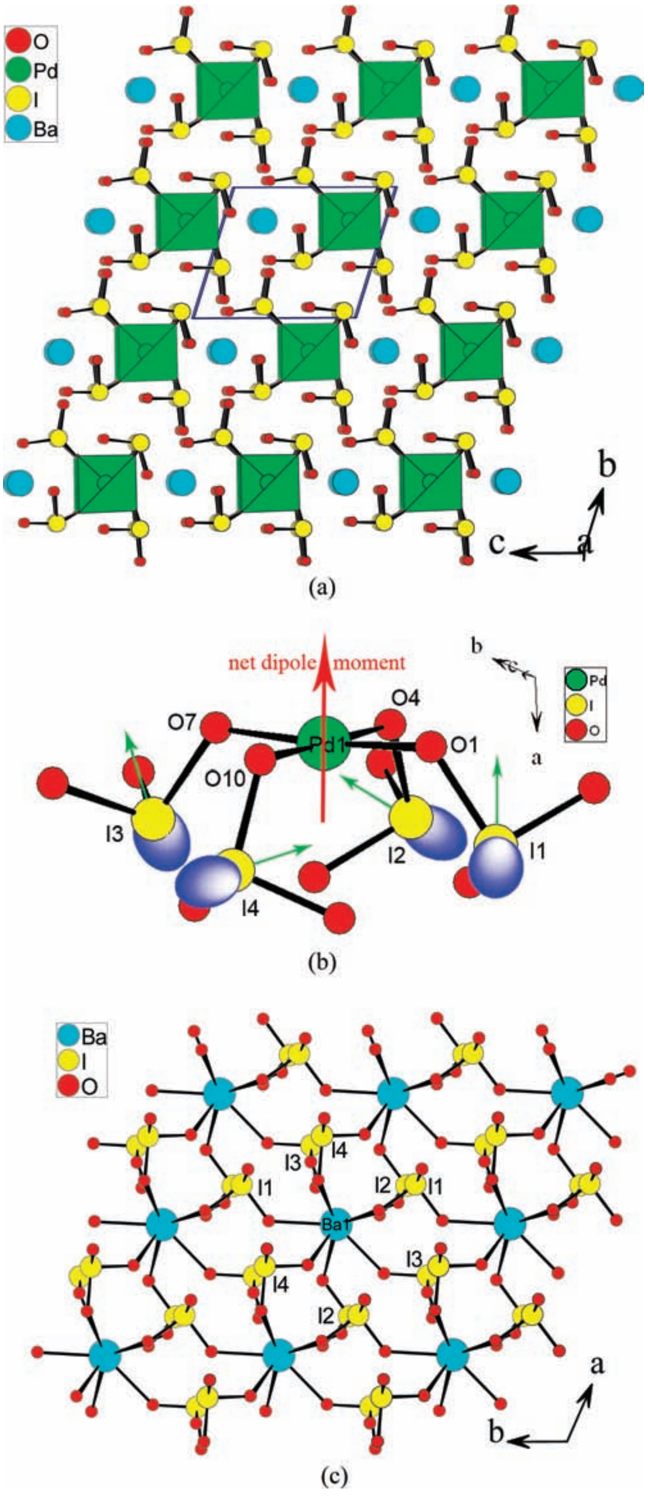

Figure 3. View of the structure of $BaPd(IO_3)_4$ down the *a*-axis (Ba−O bonds were omitted for clarity) (a); a 0D $[Pd(IO_3)]^{2-}$ unit showing the lone pairs (blue ellipsoids) and local moments (green and red arrows) (b); and a 2D $[Ba(IO_3)_4]^{2-}$ layer perpendicular to the *c*-axis (c). PdO_4 squares are shaded in green.

same direction (Figure 3b), which is similar to that in $K_{2.5}[Pd(IO_3)_4]\cdot H_{0.5}IO_3$,[18] but very different from those in $Pd(IO_3)_2$ and $AgPd(IO_3)_3$. I(1), I(2), I(3), and I(4) are away from the plane defined by O(1), O(4), O(7), and O(10) atoms 1.522, 1.635, 1.452, and 1.683 Å, respectively. Such a special arrangement of IO_3 groups results in a large net dipole moment. The packing of polar $[Pd(IO_3)_4]^{2-}$ units produces a large macroscopic net dipole moment (Figure 3a), resulting in a polar material which is confirmed also by SHG measurements as will be discussed later. In $K_{2.5}[Pd(IO_3)_4]\cdot H_{0.5}IO_3$,[18] though the $[Pd(IO_3)_4]^{2-}$ unit is polar, there is no macroscopic polarization for the 3D structure since the polarizations of neighboring $[Pd(IO_3)_4]^{2-}$ units canceled each other because of the centrosymmetric space group (*C*2/*m*).

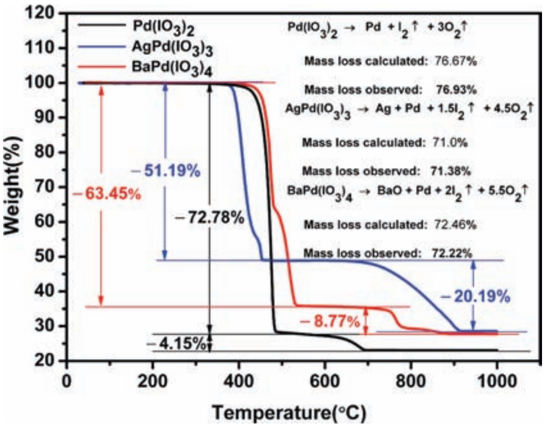

Figure 4. TGA curves for $Pd(IO_3)_2$, $AgPd(IO_3)_3$, and $BaPd(IO_3)_4$.

The Ba^{2+} cation is surrounded by eight oxygen atoms from eight unidentate iodate anions in a square antiprismatic geometry, with the Ba−O bond distances falling in the range of 2.718(12) to 3.015(12) Å. Bond valence calculations,[25] resulting in values of 2.10 for Ba, 2.21 for Pd, and 4.82−5.00 for I, indicate that the Ba, Pd, and I atoms are in an oxidation of +2, +2, and +5, respectively. The interconnection of the Ba^{2+} cations and bridging iodate anions results in a 2D $[Ba(IO_3)_4]^{2-}$ anionic layer perpendicular to the *c*-axis (Figure 3c). Neighboring such layers are interconnected by PdO_4 squares via I−O−Pd bridges into a 3D network; hence, the structure of $BaPd(IO_3)_4$ can also be described as a pillared layered structure with PdO_4 squares as pillars (Figure 3a).

Thermal Stability Studies. TGA studies indicate that $Pd(IO_3)_2$, $AgPd(IO_3)_3$, and $BaPd(IO_3)_4$ are thermally stable up to about 400, 380, and 400 °C, respectively. Then each displays two steps of weight losses (Figure 4). The weight losses in the temperature ranges 400−600, 380−490, and 400−530 °C correspond to the release of 1.0 I_2 and 2.5 O_2, 1.0 I_2 and 4 O_2, 1.8 I_2 and 4.3 O_2 per formula unit for $Pd(IO_3)_2$, $AgPd(IO_3)_3$, and $BaPd(IO_3)_4$, respectively. The residuals at 600 °C should be PdO for $Pd(IO_3)_2$, AgI and PdO for $AgPd(IO_3)_3$, $Ba_5(IO_6)_2$ and PdO for $BaPd(IO_3)_4$, respectively, which were confirmed by XRD studies (see Supporting Information, Figure S1). The observed weight losses of 72.78%, 51.19% and 63.45%, respectively for $Pd(IO_3)_2$, $AgPd(IO_3)_3$, and $BaPd(IO_3)_4$ are close to the calculated values (73.17%, 51.66%, and 63.01%). The second weight losses (600−700, 650−920, and 640−890 °C, respectively for $Pd(IO_3)_2$, $AgPd(IO_3)_3$, and $BaPd(IO_3)_4$) correspond to further decomposition of the compounds. The total weight losses at 1000 °C are 76.93%, 71.38%, and 72.22% respectively for $Pd(IO_3)_2$, $AgPd(IO_3)_3$, and $BaPd(IO_3)_4$, which are close to the calculated values (76.67%, 71.0%, and 72.46%, respectively) if the final residuals are assumed to be Pd; Ag and Pd; BaO and Pd, respectively.

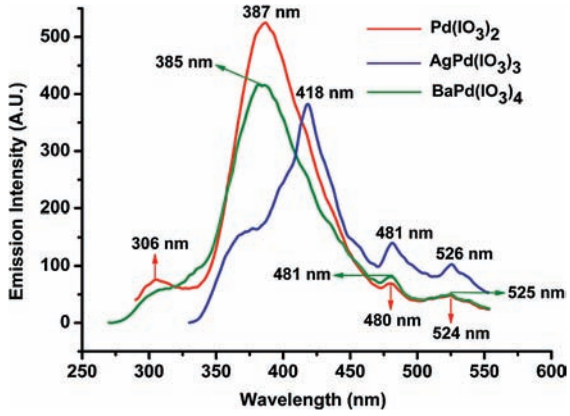

Figure 5. Solid State emission spectra of $Pd(IO_3)_2$ under $\lambda_{ex} = 242$ nm, $AgPd(IO_3)_3$ under $\lambda_{ex} = 285$ nm, and $BaPd(IO_3)_4$. under $\lambda_{ex} = 242$ nm.

The final residuals were not characterized because of their melting with the TGA bucket made of Al_2O_3 under such high temperature.

Optical Properties. IR spectra of $Pd(IO_3)_2$, $AgPd(IO_3)_3$, and $BaPd(IO_3)_4$ indicate that they are transparent in the range of 4000−900 cm^{-1} (2.5−11 μm) (Supporting Information, Figure S2). The IR absorption bands in the regions 650−837 cm^{-1} are due to I−O vibrations whereas those at 409 and 488 cm^{-1} for $Pd(IO_3)_2$, 503 cm^{-1} for $AgPd(IO_3)_3$, and 499 cm^{-1} for $BaPd(IO_3)_4$ are the characteristic absorption bands of Pd−O vibrations. These assignments are consistent with those previously reported.[10−15,18,26] UV absorption spectra of $Pd(IO_3)_2$, $AgPd(IO_3)_3$, and $BaPd(IO_3)_4$ show little absorption in the range of 1000−2500 nm (1.0−2.5 μm) (Supporting Information, Figure S3). Hence, all three compounds are transparent in the range of 1.0−11 μm. Optical diffuse reflectance spectrum studies indicate that $Pd(IO_3)_2$, $AgPd(IO_3)_3$, and $BaPd(IO_3)_4$ are semiconductors with optical band gaps of 1.31, 1.50, and 1.97 eV, respectively (Supporting Information, Figure S4).

The solid state luminescent properties of $Pd(IO_3)_2$, $AgPd(IO_3)_3$, and $BaPd(IO_3)_4$ have also been investigated at room temperature (Figure 5). Under excitation at 242 nm (for $Pd(IO_3)_2$ and $BaPd(IO_3)_4$) or 285 nm (for $AgPd(IO_3)_3$), each compound displays a strong emission band with several weak shoulder ones. The strong emission bands of $Pd(IO_3)_2$, $AgPd(IO_3)_3$, and $BaPd(IO_3)_4$ appear at 387, 418, and 385 nm, respectively, and the shoulder ones occurred at 306, 480, and 524 nm for $Pd(IO_3)_2$, 481 and 526 nm for $AgPd(IO_3)_3$, as well as 481 and 525 nm for $BaPd(IO_3)_4$, respectively. These emission bands may be associated with Pd^{2+} ions, or Ag^+ and Pd^{2+} ions, and can be assigned to the metal-centered d→s transitions as well as the metal-anion interactions.[15,27]

SHG Properties. $BaPd(IO_3)_4$ crystallized in the polar space group *P*1. Hence, it is worth studying its SHG properties. SHG measurements on a 2.05 μm Q-switch laser with the sieved powder sample (70−100 mesh) revealed that $BaPd(IO_3)_4$ displays a moderate SHG response of about 0.4× KTP ($KTiOPO_4$). On the basis of structural data, it is expected that the relative large SHG response should be derived from the unique alignments of the asymmetric IO_3 groups, that is, all of the IO_3 groups in the $[Pd(IO_3)_4]^{2-}$ unit are aligned on the same side of the distorted PdO_4 square with all of the lone pairs on I(V) atoms almost oriented in the same direction. To better understand the magnitude and direction of the dipole moments, we calculated the local dipole moments for the IO_3 polyhedra in a $[Pd(IO_3)_4]^{2-}$ unit (see Figure 3b) by using a method reported earlier.[28] With the lone-pair polyhedra, the lone-pair is given a charge of −2 and is localized 1.23 Å from the I(V) atoms.[29] The calculated magnitude of the dipole moments for IO_3 polyhedra range from 13.48 to 16.05 D (Table 3), which is consistent with previously reported values.[14c] As shown in Table 3, the *y*-component of the polarizations from all four IO_3 polyhedra is partially canceled out with a small magnitude of 6.78 D, and the positive effect comes from $I(1)O_3$ and $I(4)O_3$ polyhedra, whereas, the negative effect is derived from $I(2)O_3$ and $I(3)O_3$ polyhedra. However, both the *x*-component and *z*-component of the polarizations associated with all IO_3 polyhedra in a $[Pd(IO_3)_4]^{2-}$ unit constructively add, resulting in a large net dipole moment with the magnitudes of 28.89 and 26.27 D for the *x* and *z*-components, respectively. Such large net dipole moment should be the cause of the large SHG response. Much larger SHG response would be expected if no racemic twinning existed in the samples.

Table 3. Calculation of Dipole Moments for IO_3 Polyhedra in $BaPd(IO_3)_4$[a]

	Dipole Moment (D)			
polar unit	total magnitude	*x*-component	*y*-component	*z*-component
$I(1)O_3$	14.82	9.44	7.60	−8.53
$I(2)O_3$	13.48	2.70	−10.05	−8.57
$I(3)O_3$	16.05	15.30	−3.08	−3.75
$I(4)O_3$	13.53	1.44	12.32	−5.42
$[Pd(IO_3)_4]^{2-}$ unit		28.89	6.78	−26.27

[a] D = Debye, see also Figure 3b.

Ferroelectric Properties. The ferroelectric property of $BaPd(IO_3)_4$ was investigated because it crystallizes in a polar point group (C_1) required for ferroelectric behavior. Ferroelectric measurements revealed a very small remanent polarization (Pr) of 0.11 $\mu C/cm^2$ (Supporting Information, Figure S5); hence, the ferroelectric properties are negligible. It is unlikely that the dipole moments associated with the asymmetric IO_3 polyhedra are reversible.[11] Thus, the polarization reversibility may be limited to the small contribution from the slightly distorted PdO_4 squares or derived from dielectric loss.

Theoretical Studies. The calculated band structures of the three compounds along high symmetry points of the first Brillouin zone are plotted in Figure 6. The state energies (eV) of the lowest conduction band (L-CB) and

---

(26) Nyquist, R. A.; Kagel, R. O. *Infrared Spectra of Inorganic Compounds*; Academic Press: New York and London, 1971.

(27) (a) Ford, P. C.; Vogler, A. *Acc. Chem. Res.* **1993**, *26*, 220. (b) Che, C. M.; Tse, M. C.; Chan, M. C. W.; Cheung, K. K.; Phillips, D. L.; Leung, K. H. *J. Am. Chem. Soc.* **2000**, *122*, 2464. (c) Henary, M.; Zink, J. I. *Inorg. Chem.* **1991**, *30*, 3111. (d) Sabin, F.; Ryu, C. K.; Ford, P. C.; Vogler, A. *Inorg. Chem.* **1992**, *31*, 1941.

(28) (a) Maggard, P. A.; Nault, T. S.; Stern, C. L.; Poeppelmeier, K. R. *J. Solid State Chem.* **2003**, *175*, 27. (b) Izumi, H. K.; Kirsch, J. E.; Stren, C. L.; Poeppelmeier, K. R. *Inorg. Chem.* **2005**, *44*, 884. (c) Sivakumar, T.; Chang, H. Y.; Baek, J.; Halasyamani, P. S. *Chem. Mater.* **2007**, *19*, 4710. (d) Chang, H. Y.; Kim, S. H.; Ok, K. M.; Halasyamani, P. S. *Chem. Mater.* **2009**, *21*, 1654.

(29) Galy, J.; Meunier, G. *J. Solid State Chem.* **1975**, *13*, 142.

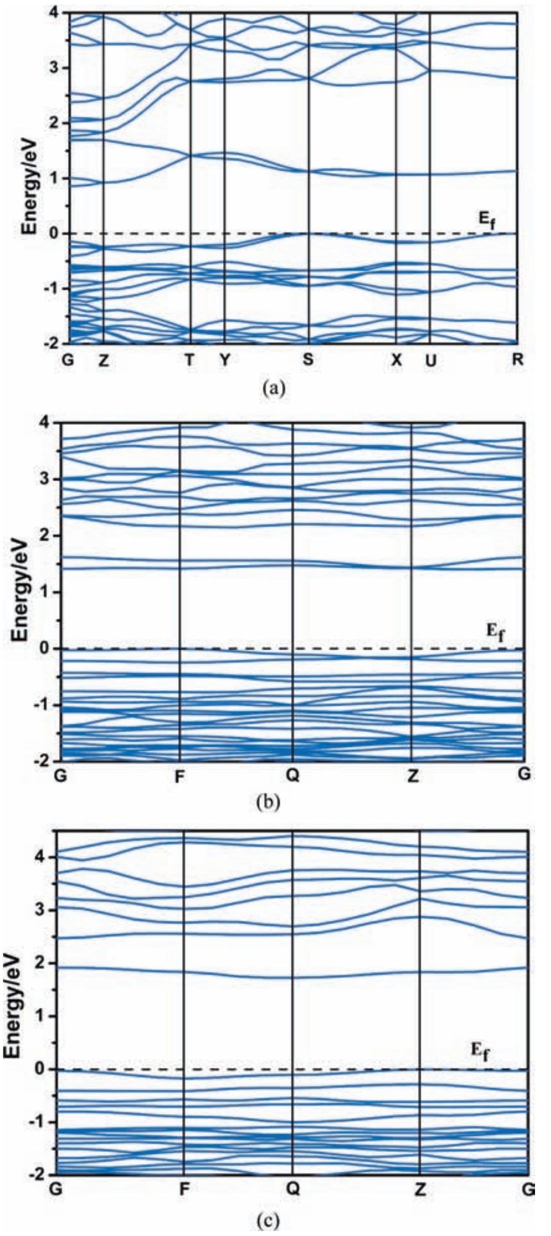

Figure 6. Band structures for the crystals $Pd(IO_3)_2$ (a), $AgPd(IO_3)_3$ (b), and $BaPd(IO_3)_4$ (c) (the Fermi level is set at 0 eV).

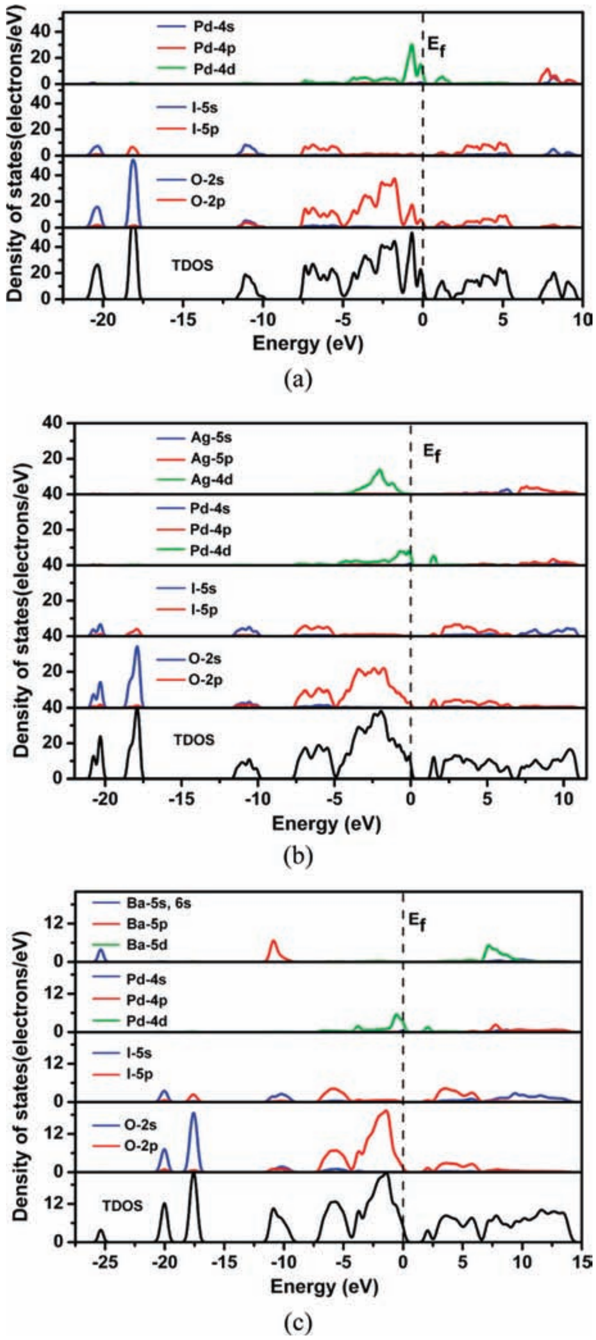

Figure 7. Total density of states and partial density of states of $Pd(IO_3)_2$ (a), $AgPd(IO_3)_3$ (b), and $BaPd(IO_3)_4$ (c) (the Fermi level is set at 0 eV).

the highest valence band (H-VB) of the compounds are listed in Supporting Information, Table S1. The calculated band structures (Figure 6 and Supporting Information, Table S1) indicate that the three compounds are all indirect band gap semiconductors with band gaps of 0.86, 1.41, and 1.73 eV for $Pd(IO_3)_2$, $AgPd(IO_3)_3$, and $BaPd(IO_3)_4$, respectively. The calculated band gaps are slightly smaller than the experimental values (1.31 eV for $Pd(IO_3)_2$, 1.50 eV for $AgPd(IO_3)_3$, and 1.97 eV for $BaPd(IO_3)_4$). This is not surprising as it is well-known that the GGA does not accurately describe the eigenvalues of the electronic states, which often causes quantitative underestimation of band gaps for semiconductors and insulators.[30]

The bands can be assigned according to the total and partial densities of states (DOS) as plotted in Figure 7. For $Pd(IO_3)_2$ [Figure 7a], the bottom-most VB region ranging from −21.5 to −17.5 eV are mainly originated from O-2s, mixing with small amount of I-5s and I-5p states. The band between −12.5 and −9.5 eV is composed of O-2s, I-5s, I-5p states. We will focus on the Fermi level region (between −8.0 and 6.0 eV), which accounts for most of the bonding character in a compound. It is obvious that O-2p states dominate the whole Fermi level region. In the regions of −8.0−(−5.0) and 1.0−6.0 eV, I-5p states overlap fully with O-2p, and in the regions of −5.0−0 and 1.0−1.8 eV, Pd-4d also overlap well with O-2p, indicating the well-defined Pd−O coordination in

---

[30] (a) Godby, R. W.; Schluther, M.; Sham, L. *J. Phys. Rev. B* **1987**, *36*, 6497. (b) Okoye, C. M. I. *J. Phys.: Condens. Matter* **2003**, *15*, 5945. (c) Terki, R.; Bertrand, G.; Aourag, H. *Microelectron. Eng.* **2005**, *81*, 514.

PdO_4 planar square and I–O covalent interactions. From Figure 7b and 7c, it is clear that the PDOSs of Pd, I and O in $AgPd(IO_3)_3$ and $BaPd(IO_3)_4$ behave very similar to those in $Pd(IO_3)_2$, and as expected, those of cations (Ag and Ba) exhibit obvious ionicity.

Conclusions

In summary, the introduction of the square-planar Pd^{2+} cations into the metal iodate systems afforded three new novel palladium(II) iodates. They represent the first examples of ternary and quaternary palladium(II) iodates and display three different structural types. Their structures feature 2D $Pd(IO_3)_2$ layer, 1D $[Pd(IO_3)_3]^-$ chain, and 0D $[Pd(IO_3)_4]^{2-}$ unit, respectively. The different alignments for the lone pairs make these materials polar or non-polar. $BaPd(IO_3)_4$ is the first polar palladium(II) iodate and displays good NLO properties. Furthermore, they also have good thermal stabilities and luminescent properties. Our future research efforts will be devoted to the explorations of other new NLO materials in the metal iodates containing a square-planar MO_4 units.

Acknowledgment. This work was supported by the National Natural Science Foundation of China (Nos. 20731006, 20825104, and 20821061), NSF of Fujian Province (No. E0420003) and Key Project of FJIRSM (No. SZD07001-2). We thank Dr. Chao He for his kind help with the ferroelectric measurements.

Supporting Information Available: X-ray crystallographic files in CIF format, simulated and experimental XRD patterns, IR, UV absorption and optical diffuse reflectance spectra. This material is available free of charge via the Internet at http://pubs.acs.org.